

# Particle size distribution in Saturn's rings: Aggregation-fragmentation model

Nikolai Brilliantov<sup>\*</sup>, Paul Krapivsky<sup>†</sup>, Anna Bodrova<sup>‡</sup>, Frank Spahn<sup>§</sup>, Hisao Hayakawa<sup>¶</sup>, Vladimir Stadnichuk<sup>‡</sup>, and Jürgen Schmidt<sup>||</sup>

<sup>\*</sup>University of Leicester, Leicester, United Kingdom, <sup>†</sup>Department of Physics, Boston University, Boston, USA, <sup>‡</sup>Moscow State University, Moscow, Russia, <sup>§</sup>University of Potsdam, Potsdam, Germany, <sup>¶</sup>Yukawa Institute for Theoretical Physics, Kyoto University, Kyoto, Japan, and <sup>||</sup>University of Oulu, Department of Physics, Oulu, Finland

Submitted to Proceedings of the National Academy of Sciences of the United States of America

Saturn's rings consist of a huge number of water ice particles, with a tiny addition of rocky material. They form a flat disk, as the result of an interplay of angular momentum conservation and the steady loss of energy in dissipative inter-particle collisions. For particles in the size range from a few centimeters to about a few meters a power law distribution of radii  $\sim r^{-q}$  with  $q \approx 3$ , has been observed by various methods [1, 2, 3, 4]. For larger sizes, the distribution steeply decays [5, 6, 7, 8] with increasing  $r$ . It has been suggested that this size distribution may arise from a balance between aggregation and fragmentation of ring particles [9, 10, 11, 12, 13, 14, 15], but to date neither the power-law dependence, nor the upper size cutoff have been explained or quantified within a unified theory. Here we present a new kinetic model for the collisional evolution of the particle size distribution which explains quantitatively space observations. In accordance with the observation data, our model predicts the exponent  $q$  to be constrained to the interval  $2.75 \leq q \leq 3.5$ . An exponential cutoff for larger particle sizes also establishes naturally with the cutoff-radius being set by the relative frequency of aggregating and disruptive collisions. This cutoff is much smaller than the typical scale of micro-structures seen in Saturn's rings ( $\sim 100$  m for self-gravity wakes) [16] and our theory represents values averaged over these structures.

Saturn's rings | planetary rings | fragmentation

## Introduction

A life-time of Saturn's rings is shorter than the age of the Saturn (Kronian) system itself [17, 18, 19], which indicates that the ring particles and their size distribution may not be primordial. Ring particles are involved in an active accretion-destruction dynamics [20] and their sizes distribute for a few decades as a power-law with a sharp cutoff for large dimensions. Tidal forces fail to explain the abrupt decay of the size distribution for house-sized particles, see [21], hence natural questions arise: (i) can the aggregation and fragmentation processes alone be responsible for the observed size distribution and (ii) whether this distribution is peculiar for Saturn's rings, or it is universal for planetary rings in general? To respond these questions quantitatively, one needs to develop a detailed model of the processes in which the rings particles are involved. Here we elaborate such model and quantify the observed properties of the particle size distribution; we show that these are generic features of a steady-state, when a balance between aggregation and fragmentation holds. Our model is based solely on the hypothesis that collisions are *binary* and that they may be classified as aggregative, restitutive and disruptive; which type of the collision is realized depends on the relative speed of colliding particles and their masses. We apply kinetic theory of granular gases [22] for the multi-component system of ring particles to quantify the collision rate and the type of an impact.

## Model

Ring particles may be treated as "dynamic ephemeral bodies" [11], built up of primary grains [13] of a certain size  $r_1$  and

mass  $m_1$ <sup>1</sup>. Let the mass of ring particles of size  $k$ , containing  $k$  primary grains, be  $m_k = km_1$  and their number density (or concentration) –  $n_k$ . For the purpose of kinetic description we assume that all particles are spheres; then the characteristic radius of an agglomerate containing  $k$  monomers scales with mass as  $r_k = r_1 k^{1/3}$ <sup>2</sup>. Dense rings composed of hard spheres can be described in the framework of the Enskog-Boltzmann theory [24, 25, 26]. In this case the rate of binary collisions depends on particle dimension and relative velocity. Namely, the cross-section for the collision of particles of size  $i$  and  $j$  can be written as  $\sigma_{ij}^2 = (r_i + r_j)^2 = r_1^2(i^{1/3} + j^{1/3})^2$ , while the relative speed, being of the order of  $0.01 - 0.1$  cm/s [3], is determined, respectively, by the velocity dispersions  $\langle \mathbf{v}_i^2 \rangle$  and  $\langle \mathbf{v}_j^2 \rangle$  for particles of size  $i$  and  $j$ . The velocity dispersion quantifies the root mean square deviation of particle velocities from the orbital speed ( $\sim 20$  km/s). These deviations follow a certain distribution, implying a range of inter-particle impact speeds, and thus, different collisional outcomes. The detailed analysis of an impact shows that for collisions at small relative velocities, when the relative kinetic energy is smaller than a certain threshold energy,  $E_{\text{agg}}$ , particles stick together to form a joint aggregate [27, 15, 28]. This occurs because adhesive forces acting between ice particles' surfaces are strong enough to keep them together. For larger velocities, particles rebound with a partial loss of their kinetic energy. For still larger impact speeds, the relative kinetic energy exceeds the threshold energy for fragmentation,  $E_{\text{frag}}$ , and particles break into pieces [28].

To illustrate the main ideas we consider here force-free dilute and spatially uniform systems. It is possible to take into account the effects of excluded volume of grains, non-homogeneity, as it is observed in self-gravity wakes, and gravitational interactions between particles. These, however, do not alter the form of the kinetic equations, which may be then formulated for the space-averaged values (see the Supporting Information).

Let  $f_i \equiv f(m_i, \mathbf{v}_i, t)$  be the mass-velocity distribution function which gives concentration of particles of mass  $m_i$

## Reserved for Publication Footnotes

<sup>1</sup>It has been recently shown that all particles with dimensions below a certain radius are absent in dense rings [23]

<sup>2</sup>In principle, the aggregates can be fractal objects, so that  $r_k \sim k^{1/D}$ , with the fractal dimension of the aggregates,  $D < 3$ . For dense planetary rings it is reasonable to assume the aggregates to be compact,  $D = 3$ .

with the velocity  $\mathbf{v}_i$  at time  $t$ . The mass-velocity distribution function evolves in a homogeneous system according to the Boltzmann equation,

$$\frac{\partial}{\partial t} f_k(\mathbf{v}_k, t) = I_k^{\text{res}} + I_k^{\text{heat}} + I_k^{\text{agg}} + I_k^{\text{frag}}. \quad [1]$$

where the right-hand side accounts for particles collisions. The first term  $I_k^{\text{res}}$  is the Boltzmann collision integral corresponding to rebound of colliding particles [22]. The second term  $I_k^{\text{heat}}$  describes the viscous heating caused by the Keplerian shear, e.g. [29]. The terms  $I_k^{\text{agg}}$  and  $I_k^{\text{frag}}$  are, respectively, the collision integrals that describe the impacts, leading to aggregation and fragmentation (the explicit expressions of all these terms are given in the Supporting information). To derive the kinetic equations for the concentrations of the species,  $n_k(t) = \int d\mathbf{v}_k f_k(\mathbf{v}_k, t)$ , one needs to integrate Eq. (1) over  $\mathbf{v}_k$ . Assuming that all species have a Maxwell velocity distribution function with average velocity  $\langle \mathbf{v}_k \rangle = 0$  and velocity dispersion  $\langle \mathbf{v}_k^2 \rangle$  we obtain (see the Supporting Information for the detail):

$$\begin{aligned} \frac{dn_k}{dt} = & \frac{1}{2} \sum_{i+j=k} C_{ij} n_i n_j - \sum_{i=1}^{\infty} C_{ki} n_i n_k \\ & - \sum_{i=1}^{\infty} A_{ki} n_i n_k (1 - \delta_{k1}) + \sum_{i=1}^k n_i \sum_{j=k+1}^{\infty} A_{ij} n_j x_k(j) \\ & + \frac{1}{2} \sum_{i,j \geq k+1} A_{ij} n_i n_j [x_k(i) + x_k(j)]. \end{aligned} \quad [2]$$

The first term in the r.h.s. of Eq. (2) describes the rate at which aggregates of size  $k$  are formed in aggregative collisions of particles  $i$  and  $j$ ; the summation extends over all  $i$  and  $j$  with  $i + j = k$ , and the factor  $\frac{1}{2}$  avoids double counting. The second and third terms give the rates at which the particles of size  $k$  disappear in collisions with other particles of any size  $i$ , due to aggregation and fragmentation, respectively. The fourth and fifth terms account for production of particles of size  $k$  due to disruption of larger bodies. Here  $x_k(i)$  is the total number of debris of size  $k$ , produced in the disruption of a projectile of size  $i$ . At first we consider a simplified collision model, assuming that both particles break completely in a disruptive collision into monomers of mass  $m_1$  which implies  $x_k(i) = i\delta_{k1}$ . As the next step we generalize our approach, assuming that the debris of fragmenting aggregates are distributed according to a more realistic model. That is, we adopt a power-law distribution of debris sizes,  $x_k(i) \sim B(i)k^{-\alpha}$ , as it is often observed in experiments, e.g. [30]. We show, however, that for steep distributions of debris, with  $\alpha > \alpha_0$ , the steady-state distribution of aggregate sizes,  $n_k = n_k(m_k)$ , is *universal*. That is, it is the same for all steep debris size distributions and coincides with  $n_k(m_k)$  for the case of complete decomposition into monomers.

The rate coefficients  $A_{ij}$  and  $C_{ij}$  (also termed as *kernels*) in the above Eq. (2) are found from kinetic theory as functions of particles sizes  $i$  and  $j$  and threshold energies  $E_{\text{agg}}$  and  $E_{\text{frag}}$ :

$$\begin{aligned} C_{ij} &= \nu_{ij} (1 - (1 + B_{ij} E_{\text{agg}}) \exp(-B_{ij} E_{\text{agg}})) \\ A_{ij} &= \nu_{ij} \exp(-B_{ij} E_{\text{frag}}) \\ \nu_{ij} &= 4\sigma_{ij}^2 \sqrt{\frac{\pi}{3} \left( \frac{\langle E_i \rangle}{m_i} + \frac{\langle E_j \rangle}{m_j} \right)} \\ B_{ij} &= \frac{3}{2} \frac{m_i + m_j}{\langle E_i \rangle m_j + \langle E_j \rangle m_i}. \end{aligned} \quad [3]$$

Here  $\langle E_i \rangle$  is the average kinetic energy of species of size  $i$ :

$$\langle E_i \rangle = \frac{1}{n_i} \int \frac{1}{2} m_i \mathbf{v}_i^2 f_i(\mathbf{v}_i) d\mathbf{v}_i = \frac{1}{2} m_i \langle \mathbf{v}_i^2 \rangle. \quad [4]$$

### Collisional fragmentation into monomers

In the case of monomer decomposition,  $x_k(i) = i\delta_{1k}$ , the kinetic equations (2) can be written in the following form:

$$\frac{dn_k}{dt} = \frac{1}{2} \sum_{i+j=k} C_{ij} n_i n_j - \sum_{i \geq 1} (C_{ik} + A_{ik}) n_i n_k \quad [5]$$

$$\begin{aligned} \frac{dn_1}{dt} &= -n_1 \sum_{j \geq 1} C_{1j} n_j + n_1 \sum_{j \geq 2} j A_{1j} n_j \\ &+ \frac{1}{2} \sum_{i,j \geq 2} A_{ij} (i + j) n_i n_j. \end{aligned} \quad [6]$$

Similar equations with terms responsible for the spontaneous fragmentation of aggregates have been analyzed previously in the context of rain drop formation [31, 32]. Although the above set of equations is still very complicated, one can obtain analytical solutions in some important for application cases.

**Constant kernels.** First we consider the simplest case of constant kinetic coefficients  $A_{ij}$  and  $C_{ij}$ . In this case  $\lambda = A_{ij}/C_{ij}$ , which characterizes the ratio of fragmentative and aggregative collisions is also constant. Denote by  $N(t) = \sum_{j=1}^{\infty} n_j(t)$  the total aggregate number density and by  $M = \sum_{k=1}^{\infty} k n_k(t)$  their total mass. Using the appropriate rescaling of time, number density and mass, we can adopt, without the loss of generality,  $C_{ij} = 1$ ,  $N(0) = 1$  and  $M = 1$ ; note that  $M$  is conserved. In this case Eqs. (5)-(6) simplify to

$$\frac{dn_1}{dt} = -n_1 N + \lambda(1 - n_1)N \quad [7]$$

$$\frac{dn_k}{dt} = \frac{1}{2} \sum_{i+j=k} n_i n_j - (1 + \lambda) n_k N. \quad [8]$$

Summing Eqs. (7)-(8) we arrive at a closed ordinary differential equation for the aggregate density  $N(t)$ , which is solved to yield

$$N(t) = \frac{2\lambda}{1 + 2\lambda - e^{-\lambda t}}. \quad [9]$$

For concreteness, we consider the mono-disperse initial condition:  $n_k(t=0) = \delta_{k,1}$ . Plugging Eq. (9) into Eq. (7) and solving the resulting equation we obtain

$$n_1(t) = \lambda_1 \left[ 1 + \lambda^{-1} \left( \lambda_2^{-1} e^{\lambda t} - \lambda^{-1}/2 \right)^{-\lambda_2/\lambda_1} \right], \quad [10]$$

with  $\lambda_1 = \lambda/(1 + \lambda)$  and  $\lambda_2 = 2\lambda/(1 + 2\lambda)$ . Utilizing the recursive nature of Eqs. (8) one can find  $n_k(t)$  with  $k > 1$ . The consecutive equations quickly get very unwieldy as the mass  $k$  grows. Hence we limit ourselves to the asymptotic behavior. After a relaxation time that scales as  $\lambda^{-1}$ , the system approaches to a non-trivial steady state, with  $n_1 = \lambda_1$  and  $N = \lambda_2$ , while the steady concentrations  $n_k$  for  $k \geq 2$  are determined by the equation,

$$0 = \frac{1}{2} \sum_{i+j=k} n_i n_j - (1 + \lambda) n_k N. \quad [11]$$

Introducing the generating function  $\mathcal{N}(z) = \sum_{k \geq 1} n_k z^k$ , we convert the stationary equation Eqs. (11) into an algebraic equation

$$\mathcal{N}(z)^2 - 2(1 + \lambda)N\mathcal{N}(z) + 2(1 + \lambda)Nn_1z = 0 \quad [12]$$

for the generating function. Its solution reads:

$$\mathcal{N}(z) = (1 + \lambda) N \left[ 1 - \sqrt{1 - \frac{2n_1}{(1 + \lambda)N} z} \right]. \quad [13]$$

Expanding  $\mathcal{N}(z)$  we arrive at

$$n_k = \frac{N}{\sqrt{4\pi}} (1 + \lambda) \left[ \frac{2n_1}{(1 + \lambda)N} \right]^k \frac{\Gamma(k - \frac{1}{2})}{\Gamma(k + 1)}. \quad [14]$$

The above relation may be further simplified taking into account that for the most of the rings' particles  $k \gg 1$ . Using the steady state values of  $N$  and  $n_1$  and additionally assuming that  $\lambda \ll 1$ , we obtain

$$n_k = \frac{\lambda}{\sqrt{\pi}} e^{-\lambda^2 k} k^{-3/2}. \quad [15]$$

Thus in the region  $k < \lambda^{-2}$ , the mass distribution exhibits a power-law dependence with an exponential cutoff for larger  $k$ .

**Generalized Product Kernels.** Although the above result (15) provides an important insight into the general structure of the solution of Eqs. (5) – (6), the assumption that the kinetic coefficients  $A_{ij}$ ,  $C_{ij}$  are constant is obviously an oversimplification. A more adequate description may be achieved using Eqs. (3) for the kinetic coefficients, along with the appropriate models for the quantities  $E_{\text{agg}}$ ,  $E_{\text{frag}}$  and  $\langle E_k \rangle$ . Here we study a few basic (limiting) cases and expect that these reflect the most general features of the system. Hence we consider the following two limits:

1. First, assume energy equipartition for particles of all sizes,  $\langle E_k \rangle = \text{const}$ , which physically means that energy of random motion is equally distributed among all species, like in molecular gases. We also assume that the threshold energies of aggregation and fragmentation are constant:  $E_{\text{agg}} = \text{const}$  and  $E_{\text{frag}} = \text{const}$ ; the latter quantities may be treated as effective average values for all collisions. In this case from Eqs. (3) follows that  $\lambda = A_{ij}/C_{ij} = \text{const}$  and the kinetic coefficients read

$$C_{ij} = C_0 \left( i^{1/3} + j^{1/3} \right)^2 \left( i^{-1} + j^{-1} \right)^{1/2}, \quad [16]$$

where  $C_0 = \text{const}$ . Note that the coefficients  $C_{ij}$  are homogeneous functions of masses of colliding particles  $m_i \sim i$  and  $m_j \sim j$ , that is, if  $a$  is some positive number, then

$$C_{ai aj} = a^\varkappa C_{ij} \quad [17]$$

where  $\varkappa = 1/6$  is the homogeneity degree.

2. Second, somewhat opposite case corresponds to equal velocity dispersion for all species,  $\langle \mathbf{v}_i^2 \rangle = \mathbf{v}_0^2 = \text{const}$ , which implies the same magnitude of random velocity for small and large particles. Let us also assume the limiting size dependence of the fragmentation threshold energy  $E_{\text{frag}}$ . Namely, we assume that  $E_{\text{frag}}$  is proportional to the mass of the colliding aggregates, that is, to  $m_i$  or to  $m_j$ . Here we employ a symmetrized dependence,  $E_{\text{frag}} = E_0 (ij)/(i + j)$ , with  $E_0 = \text{const}$  which yields  $B_{ij} E_{\text{frag}} = \left( \frac{3E_0}{2m_1 \mathbf{v}_0^2} \right) = \text{const}$  and allows a simplified analysis. Furthermore, we assume that the aggregation threshold energy  $E_{\text{agg}}$  for all colliding pairs is large compared to the average kinetic energy of the relative motion,  $\frac{1}{2} \mu_{ij} \mathbf{v}_0^2$  with  $\mu_{ij} = m_1 (ij)/(i + j)$ . Then  $B_{ij} E_{\text{agg}} \gg 1$  and from Eqs. (3) we obtain  $C_{ij} = \nu_{ij}$  and therefore  $\lambda = A_{ij}/C_{ij} = \exp(-B_{ij} E_{\text{frag}}) = \text{const}$ . The kinetic coefficients attain in this case the following form,

$$C_{ij} = \tilde{C}_0 \left( i^{1/3} + j^{1/3} \right)^2, \quad [18]$$

were again  $\tilde{C}_0 = \text{const}$ , and  $C_{ij}$  are homogeneous functions of  $i$  and  $j$  of the homogeneity degree  $\varkappa = 2/3$ . Note that the detailed analysis (see the Supporting Information) of the aggregation threshold energy  $E_{\text{agg}}$ , based on the theory of dissipative collisions of adhesive particles [33], showed that for the characteristic random velocity in the rings (of the order of a few millimeters per second [3]), the assumed condition  $B_{ij} E_{\text{agg}} \gg 1$  is fulfilled for almost all collisions.

An important property of the kinetic equations, where the kinetic coefficients  $C_{ij}$  and  $A_{ij} = \lambda C_{ij}$  (with constant  $\lambda$ ) are homogeneous functions of the sizes of colliding particles  $i$  and  $j$ , is that these equations possess a scaling solution for  $i, j \gg 1$ ; the latter is mainly determined by the homogeneity degree  $\varkappa$  but not by the detailed form of these coefficients [34, 35]. We use this property and replace the original rate coefficients (16) and (18) by the simplified ones,

$$C_{ij} = \hat{C}_0 (ij)^\mu \quad \hat{C}_0 = \text{const} \quad [19]$$

where the homogeneity degree  $\varkappa = 2\mu$  and  $\mu = 1/12$  for the first limiting case and  $\mu = 1/3$  for the second. The advantage of this simplified kernel is the existence on an analytic solution for the steady state distribution. Indeed, with the homogeneous coefficients (19) the steady-state version of Eqs. (5) reads,

$$0 = \frac{1}{2} \sum_{i+j=k} l_i l_j - (1 + \lambda) l_k L \quad [20]$$

where we have used the shorthand notations

$$l_k = k^\mu n_k, \quad L = \sum_{k \geq 1} l_k. \quad [21]$$

With the substitute,  $n_k \rightarrow l_k$  and  $N \rightarrow L$ , the system of equations (20) is mathematically identical to the system of equations with a constant kernel (11). Hence we straightforwardly obtain,

$$n_k = \frac{L}{2\sqrt{\pi}} e^{-\lambda^2 k} k^{-3/2-\mu}, \quad [22]$$

which is again a power-law dependence with the exponential cutoff. To verify the validity of various approximations made to obtain the above analytical solution, we perform a numerical analysis. We directly solve the system of rate equations (5) – (6) for both limiting kernels (16) and (18), together with their simplified counterparts (19), see Fig. 1. As it follows from the figure the stationary distributions for the systems with the complete kinetic coefficients (16) – (18) have exactly the same slope as the systems with the simplified kernel (19) of the same degree of homogeneity. Similarly, the exponential cutoff in the particles' size distribution is observed for both systems – with complete and simplified kernels. Hence we conclude that the simplified power-law coefficients (19) may be used for the *quantitative* description of the dominant part of the size distribution.

Note that the above kernels (16) and (18) with the homogeneity degree  $2\mu = 1/6$  and  $2\mu = 2/3$  correspond to the limiting cases for the size dependence of the average energy of the rings' particles,  $\langle E_k \rangle \sim k^\beta$  for  $\beta = 0$  and  $\beta = 1$ . Physically, we expect that  $\beta$  is constrained within the interval  $0 \leq \beta \leq 1$ . Indeed, if  $\beta$  was negative, this would imply that very big particles have vanishing velocity dispersion, which is only possible for unrealistic condition of the collision-free motion. The condition  $\beta > 1$  is unrealistic as well, since it would imply that the energy, pumped in due to collisions, increases with particle mass faster than linearly; there is no evidence for such processes. Applying this physically plausible arguments, we conclude that  $\beta$  must be limited within the interval  $[0, 1]$ , and therefore  $\mu$  obeys the restrictions  $1/12 \leq \mu \leq 1/3$ .

## Other fragmentation models.

### Universality condition for the resultant size-distribution

As it has been shown above, the complete breakage of rings' particles in collisions into monomers, leads to a power-law steady-state size distribution. A more realistic fragmentation model corresponds however to a power-law size distribution of debris [30], that is, the number of debris of size  $k$  produced in fragmentation of particle of size  $i$  scales as  $x_k(i) \sim B(i)/k^\alpha$  [see Eqs. (2)]. Intuitively, one expects that if the distribution of the debris size is steep enough, so that small fragments dominate, the resultant steady-state distribution of the rings particles will be close to that for the complete fragmentation into monomers. A scaling analysis, outlined below confirms this assumption; it also indicates that for  $\alpha > 2$  (steep debris-size distributions)  $x_k(i) \sim i/k^\alpha$  (see the Supporting Information for more detail).

Substituting the power-law distribution for debris size,  $x_k(i) \sim i/k^\alpha$ , into the basic kinetic equations (2), we notice that the obtained equations are very similar to the already studied for case of complete fragmentation into monomers. Indeed, if  $\alpha > 2$ , so that  $x_k(i) \sim i/k^\alpha$ , the equation for the monomer concentration  $n_1$  is identical to Eq. (6), up to a factor at the coefficients  $A_{ij}$ . At the same time, the equations for  $n_k$  have the same terms as the respective Eqs. (5) plus two extra terms, corresponding to the forth and fifth terms in the basic Eqs. (2). These describe the additional input of particles, composed of  $k$  monomers, due to decomposition of larger aggregates. If we assume that the steady-state distribution has the same form as for monomer decomposition,  $n_k \sim k^{-\gamma} e^{-ak}$ , one can estimate (up to a factor) these additional terms for the case of homogeneous kinetic coefficients,  $A_{ij} = \lambda C_{ij} \sim (ij)^\mu$  [see Eq. (19)], as:

$$\sum_{i=1}^k \sum_{j=k+1}^{\infty} A_{ij} n_i n_j B(j) k^{-\alpha} \sim k^{-\alpha} \quad [23]$$

$$\frac{1}{2} \sum_{i,j \geq k} A_{ij} n_i n_j [B(i) + B(j)] k^{-\alpha} \sim k^{\mu-\gamma+1-\alpha}, [24]$$

where we also assume that  $ka \ll 1$ , which corresponds to the power-law domain of the size distribution. The above terms are to be compared with the other three terms in Eqs. (2) or Eqs. (5), which are the same for the both models – of monomer decomposition or power-law fragmentation,

$$\frac{1}{2} \sum_{i+j=k} C_{ij} n_i n_j \sim \sum_{i \geq 1} C_{ik} n_i n_k \sim \sum_{i \geq 1} A_{ik} n_i n_k \sim k^{\mu-\gamma}. \quad [25]$$

Obviously, if the new, additional terms (23) and (24) are negligible, as compared to the terms (25), that are the same for the both models, the resultant steady-state size distribution would be the same as well. For large  $k \gg 1$ , which is the case of interest, one can neglect the terms (23) and (24) as compared to (25) if  $\alpha > \gamma - \mu$  and  $\alpha > 1$ . If we also take into account that the equations for the monomers for the two models coincide for  $\alpha > 2$ , we conclude, that the condition of the universality of the steady-state distribution reads,  $\alpha > \max\{\gamma - \mu, 2\}$ .

In the case of monomer decomposition  $\gamma = \mu + 3/2$ , or  $\gamma - \mu = 1.5$ , as it follows from Eq. (22). Hence the above condition implies  $\alpha > 2$ . In other words, if  $\alpha > 2$ , the model of the complete decomposition into monomers yields the same resultant particle size distribution as the model with any power-law distribution of debris. Moreover, it may be shown (see the Supporting Information) that the steady-state

size-distribution of aggregates (22) is generally *universal*: It is the same for all size distributions of debris, with a strong dominance of small fragments, independently of its functional form. We check this conclusion numerically, solving the kinetic equations (2) with the the power-law and exponential size distribution of debris, see Fig. 2. As it follows from the figure, the particle size distribution (22) is indeed universal for steep distributions of debris size. Fig. 2 also confirms the condition of universality of distribution (22),  $\alpha > 2$ , for power-law debris size-distributions.

Note that a steep distribution of debris size, with strong domination of small fragments seems very plausible from the physical point of view: The aggregates are relatively loose objects, with a low average coordination number, that is, with a small number of bonds between neighboring constituents. It is much easier to break into small pieces such objects, than solids or aggregates with a large coordination number.

### Particles' radii distribution: Theory and observations

To obtain the radii distribution of rings particles,  $F(R)$ , which is constrained by space observations, we use the relation  $R^3 = r_k^3 = k r_1^3$  (for spherical particles) in conjunction with  $n_k dk = F(R) dR$ . We find that  $n_k \sim k^{-3/2-\mu}$  implies

$$F(R) \sim R^{-q} e^{-(R/R_c)^3} \quad q = 5/2 + 3\mu \quad [26]$$

$$R_c = r_1 / \lambda^{2/3}, \quad [27]$$

that is, for  $R \ll R_c$  the distribution obeys a power-law with the exponent  $q = 5/2 + 3\mu$  and for larger radii,  $R \sim R_c$  it has an exponential cutoff.

The exponent  $\mu$  can vary within the interval,  $1/12 \leq \mu \leq 1/3$ , and hence the exponent  $q$  for the radii distribution varies in the range  $2.75 \leq q \leq 3.5$ . This is in the excellent agreement with observations of the spacemissions of Saturn (Voyager, Cassini), where values for  $q$  in the range from 2.70 to 3.11 were reported [2, 4]. We have performed the fitting of the the particle size distribution of Saturn's A ring inferred from data obtained by the Voyager Radio Science Subsystem (RSS) during a radio occultation of the spacecraft by the rings, using the distribution (26), see Fig. 3. As it follows from the figure, the space observation data are in a perfect agreement with our theory.

## Conclusions

We have developed a new generalized kinetic model, where the steady-state distribution of particles' size results from the dynamic balance between aggregation and fragmentation processes. The model explains quantitatively the particle size-distribution of Saturn's rings, observed by several space-missions (Voyager, Cassini). It gives naturally a power-law size distribution with a correct slope as well as a large-size cutoff. Interestingly, the exponent of the power-law,  $q = 2.5 + 3\mu$  is a sum of two parts. The main part, 2.5, corresponds the basic case, when the collision frequency does not depends on particle size ( $\mu = 0$ ); such slope is generic for a size-distribution when aggregation-fragmentation balance holds for *binary* collisions. The additional part  $3\mu$  from the interval  $0.25 \leq 3\mu \leq 1$  characterizes size dependence of the impact frequency. The latter is determined by the particles diameters and the kinetic energy of their random motion. We obtain analytical solutions for the limiting cases of kinetic energy equipartition,  $\langle E_k \rangle = \text{const}$ , ( $3\mu = 0.25$ ) and of equal velocity dispersion for all species  $\langle \mathbf{v}_k^2 \rangle = \text{const}$ , ( $3\mu = 1$ ). These give the limiting slopes of  $q = 2.75$  and  $q = 3.5$ . Physically, we expect that any intermediate dependence between

these two limiting cases may realize, which would possibly imply the power-law size distribution with the exponent within the interval  $2.75 \leq q \leq 3.5$ .

Note that the obtained rather general results follow directly from a few basic assumptions: (i) ring-particles are aggregates comprised by primary grains, kept together by adhesive (or gravitational) forces, (ii) the aggregate sizes change due to *binary* collisions, which are aggregative, restitutive, or fragmentative and (iii) the collision rate and a type of an impact are determined by the distribution of random velocities of the ring-aggregates. We wish to stress that the power-law distribution with a cutoff is a *direct mathematical consequence* of the above assumptions only, that is, there is no need to *suppose* a power-law distribution and search for an additional mechanism for a cutoff, as in the previous semi-quantitative approach of Ref. [13].

The agreement between the observations of the space-probes Voyager and Cassini and predictions of our model for the aggregate's size-distribution indicates that dense planetary rings are indeed mainly composed of so-called ephemeral dynamical bodies (DEB), suggested already three decades ago [10, 11]. This means that the (ice) aggregates constituting the cosmic disks permanently change their mass due to collision-caused aggregation and fragmentation, while their distribution of sizes remains stationary. In other words, the results of our study provide another (quantitative) proof that the particle size distribution of Saturn rings is not primordial.

Moreover, one expects the same size distribution for other non-primordial rings.

The predictive power of the kinetic model further emphasizes the role of adhesive contact forces between constituents which dominate for aggregate sizes up to the observed cutoff radius of  $R_c \sim 5 - 10$  m. The model does not describe the largest constituents in the rings, with sizes beyond  $R_c$ . These are the propeller-moonlets in the A and B rings of Saturn and their origin is believed to be the result of a catastrophic disruption [20]. We also do not discuss the nature of the smallest constituents, that is, of the primary grains. These particles are probably themselves comprised of still smaller entities and correspond to the least-size free particles observed in the rings (see Ref. [23] for detail).

Our model gives the upper cutoff radius  $R_c$  in terms of the primary grain radius and the ratio of the fragmentative and aggregative collisions, Eq. (27). Since this ratio increases with increasing kinetic energy of particles' random motion, the cutoff radius is expected to be smaller for rings with larger velocity dispersion. To check quantitatively this prediction of the model is the goal of our future research.

**ACKNOWLEDGMENTS.** We thank Larry Esposito, Heikki Salo, Miodrag Sremčević and Martin Seiß for fruitful discussions. Numerical calculations were performed using Chebyshev supercomputer of Moscow State University. This work was supported by Deutsches Zentrum für Luft und Raumfahrt, Deutsche Forschungsgemeinschaft, Russian Foundation for Basic Research (RFBR, project 12-02-31351). The authors also acknowledge the partial support through the EU IRSES DCP-PhysBio N269139 project.

- Marouf, E. A., Tyler, G. L., Zebker, H. A., Simpson, R. A. & Eshleman, V. R. Particle size distributions in Saturn's rings from Voyager 1 radio occultation. *Icarus* 54, 189–211 (1983).
- Zebker, H. A., Marouf, E. A. & Tyler, G. L. Saturn's rings - Particle size distributions for thin layer model. *Icarus* 64, 531–548 (1985).
- Cuzzi, J. et al. Ring Particle Composition and Size Distribution, 459–509 (Springer, 2009).
- French, R. G. & Nicholson, P. D. Saturn's Rings II. Particle sizes inferred from stellar occultation data. *Icarus* 145, 502–523 (2000).
- Zebker, H. A., Tyler, G. L. & Marouf, E. A. On obtaining the forward phase functions of Saturn ring features from radio occultation observations. *Icarus* 56, 209–228 (1983).
- Tiscareno, M. S. et al. 100-metre-diameter moonlets in Saturn's A ring from observations of 'propeller' structures. *Nature* 440, 648–650 (2006).
- Sremčević, M. et al. A Belt of Moonlets in Saturn's A ring. *Nature* 449, 1019–1021 (2007).
- Tiscareno, M. S., Burns, J. A., Hedman, M. M. & Porco, C. C. The Population of Propellers in Saturn's A Ring. *The Astronomical Journal* 135, 1083–1091 (2008).
- Harris, A. W. Collisional breakup of particles in a planetary ring. *Icarus* 24, 190–192 (1975).
- Davis, D. R., Weidenschilling, S. J., Chapman, C. R. & Greenberg, R. Saturn ring particles as dynamic ephemeral bodies. *Science* 224, 744–747 (1984).
- Weidenschilling, S. J., Chapman, C. R., Davis, D. R. & Greenberg, R. Ring particles - Collisional interactions and physical nature. In *Planetary Rings*, 367–415 (1984).
- Gorkavyi, N. & Fridman, A. M. *Astronomy Letters* 11, 628 (1985).
- Longaretti, P. Y. Saturn's main ring particle size distribution: An analytic approach. *Icarus* 81, 51–73 (1989).
- Canup, R. M. & Esposito, L. W. Accretion in the Roche zone: Coexistence of rings and ring moons. *Icarus* 113, 331–352 (1995).
- Spahn, F., Albers, N., Sremčević, M. & Thornton, C. Kinetic description of coagulation and fragmentation in dilute granular particle ensembles. *Europhysics Letters* 67, 545–551 (2004).
- Colwell, J. E. et al. The Structure of Saturn's Rings, 375 (Springer, 2009).
- Cuzzi, J. N. & Durisen, R. H. Bombardment of planetary rings by meteoroids - General formulation and effects of Oort Cloud projectiles. *Icarus* 84, 467–501 (1990).
- Colwell, J. E. The disruption of planetary satellites and the creation of planetary rings. *Planetary and Space Science* 42, 1139–1149 (1994).
- Cuzzi, J. N. e. a. An Evolving View of Saturn's Dynamic Rings. *Science* 327, 1470–1475 (2010).
- Esposito, L. *Planetary Rings* (2006).
- Guimaraes, A. H. F. et al. Aggregates in the strength and gravity regime: Particles sizes in saturn's rings. *Icarus* 220, 660–678 (2012).
- Brilliantov, N. V. & Pöschel, T. *Kinetic Theory of Granular Gases* (Oxford University Press, Oxford, 2004).
- Bodrova, A., Schmidt, J., Spahn, F. & Brilliantov, N. Adhesion and collisional release of particles in dense planetary rings 218, 60–68 (2012).
- Araki, S. & Tremaine, S. The dynamics of dense particle disks. *Icarus* 65, 83–109 (1986).
- Araki, S. The dynamics of particle disks. II. Effects of spin degrees of freedom. *Icarus* 76, 182–198 (1988).
- Araki, S. The dynamics of particle disks III. Dense and spinning particle disks. *Icarus* 90, 139–171 (1991).
- Dominik, C. & Tielens, A. G. G. The Physics of Dust Coagulation and the Structure of Dust Aggregates in Space. *Astrophys. J.* 480, 647 (1997).
- Wada, K. Collisional Growth Conditions for Dust Aggregates. *Astrophys. J.* 702, 1490–1501 (2009).
- Schmidt, J., Ohtsuki, K., Rappaport, N., Salo, H. & Spahn, F. Dynamics of Saturn's Dense Rings, 413–458 (Springer, 2009).
- Astrom, J. A. Statistical models of brittle fragmentation. *Advances in Physics* 55, 247–278 (2006).
- Srivastava, R. C. *J. Atom. Sci.* 39, 1317 (1982).
- Hayakawa, H. Master Thesis, Kobe University (1988).
- Brilliantov, N. V., Albers, N., Spahn, F. & Pöschel, T. Collision dynamics of granular particles with adhesion. *Phys. Rev. E* 76, 051302 (2007).
- Leyvraz, F. Scaling theory and exactly solved models in the kinetics of irreversible aggregation. *Physics Reports* 383, 95–212 (2003).
- Krapivsky, P. L., Redner, A. & Ben-Naim, E. *A Kinetic View of Statistical Physics* (Cambridge University Press, Cambridge, UK, 2010).

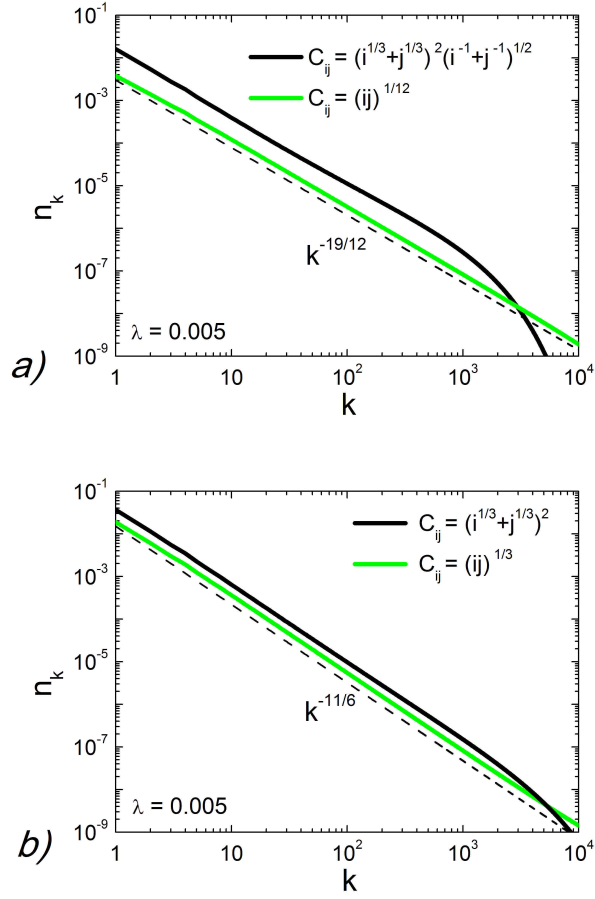


**Fig. 1. Particle size distribution for the collisional decomposition into monomers.** (a) The limiting case of energy equipartition  $\langle E_k \rangle = \text{const}$  for all species. The solid black line corresponds to the system with the complete kinetic coefficients (16), while the solid green line – to the simplified coefficients (19) with the same degree of homogeneity,  $2\mu = 1/6$ . The dashed line has the slope  $n_k \propto k^{-19/12}$ , predicted by the theory. (b) The limiting case of equal velocity dispersion for all species,  $\langle v_k^2 \rangle = \text{const}$ . The solid black line refers to the system with the complete kinetic coefficients (18), while the solid green line – to the simplified coefficients (19) with the same degree of homogeneity,  $2\mu = 2/3$ . The dashed line shows the theoretical dependence,  $n_k \propto k^{-11/6}$ . In all cases the power-law distribution turns into an abrupt exponential decay for large particles sizes.

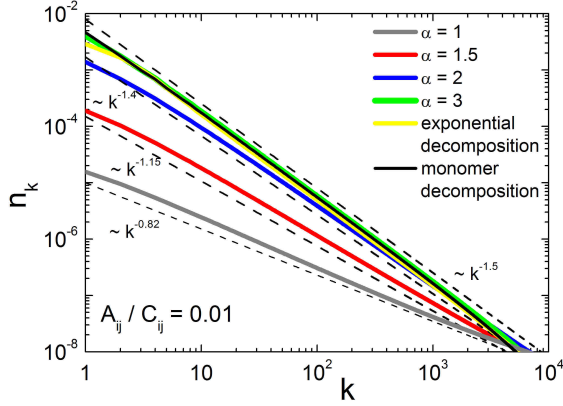


**Fig. 2. Particle size distribution for the collisional decomposition into fragments with other size distributions.** The black solid line depicts the particle size distribution for the case of monomers decomposition. The other solid lines show the resultant steady-state distributions of aggregates for the following distributions of debris size: the power-law distribution,  $x_k(i) \sim k^{-\alpha}$ , with  $\alpha = 1$  (gray),  $\alpha = 1.5$  (red),  $\alpha = 2$  (blue),  $\alpha = 3$  (green) and exponential distribution  $x_k(i) \sim \exp(-k)$  (yellow). The dashed lines indicate the corresponding fitting  $n_k \sim k^{-\gamma}$ . Note that for steep size distributions of debris ( $\alpha > 2$  and exponential distribution) all slopes coincide with the one for the case of complete decomposition into monomers. All data correspond to the systems with constant kinetic coefficients.

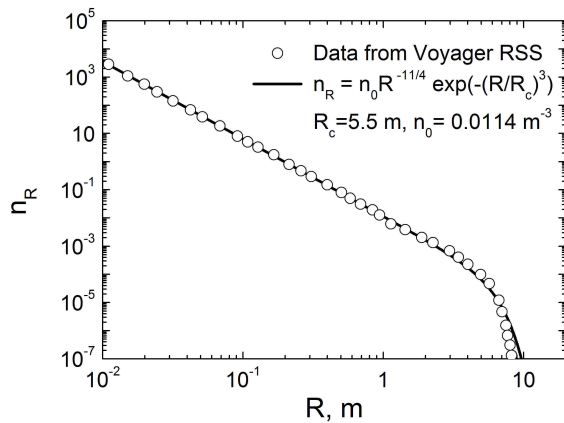


**Fig. 3. Particle size distribution for Saturn's A ring.** Symbols represent the particle size distribution of Saturn's A ring inferred from data obtained by the Voyager Radio Science Subsystem (RSS) during a radio occultation of the spacecraft by the rings [2]. A fit of the theoretical curve, Eq.(26), is shown as a solid line. A cutoff radius of  $R_c = 5.5$  m, obtained from the fit agrees well with the observation data [2].